

Thermophysical Properties of Containerless Liquid Iron up to 2500 K¹

G. Wille,^{2, 3} F. Millot,² and J. C. Rifflet²

Thermophysical properties of high temperature liquid iron heated with a CO₂ laser have been determined in an aerodynamic levitation device equipped with a high-speed camera and a three-wavelength pyrometer. Characteristic curves of the free cooling and heating of the drop can be used to determine the same apparent emissivity of solid and liquid iron and to calibrate pyrometers based on the known value of the melting point of iron, i.e., 1808 K. Examination of the recalescence of undercooled liquid iron and further solidification are used to obtain the ratio of the melting enthalpy versus the heat capacity of liquid iron as $\frac{\Delta H_m}{c_p^l} = 306 \pm 2.5$ K. The surface tension σ was determined from an analysis of the vibrations of liquid drops. Results are accurately described by σ (mJ·m⁻²) = $(1888 \pm 31) - (0.285 \pm 0.015)(T - T_m)$ between 1750 K (undercooled liquid) and 2500 K. The density of liquid iron has been deduced from the image size and the mass of the liquid iron drops.

KEY WORDS: density; levitation; liquid iron; melting enthalpy; specific heat; surface tension.

1. INTRODUCTION

Liquid iron properties have been studied extensively for obvious reasons. Recently, electromagnetic levitation techniques have proved to be useful to acquire these data without pollution. In particular, the surface tension which is important for many industrial processes has been determined for temperatures between 1750 and 2000 K [1–6].

¹ Paper presented at the Sixth International Workshop on Subsecond Thermophysics, September 26–28, 2001, Leoben, Austria.

² CRMHT/CNRS, 1D Avenue de la Recherche Scientifique, 45071 Orléans Cedex 2, France.

³ To whom correspondence should be addressed. E-mail: wille@cnrs-orleans.fr

Other levitation techniques have also been developed recently [7–10] and have been used successfully to determine thermophysical property data. Among these techniques, aerodynamic levitation associated with CO_2 laser heating is particularly promising because of its simplicity, robustness, and versatility. It has been shown by us [10, 11] that this levitation technique is quite well adapted to the measurement of the density and surface tension of liquids up to 3500 K in appropriate cases.

This paper reports on some properties of liquid iron in the temperature range 1700 to 2500 K determined in an aerodynamic levitation setup. The results are critically compared with literature results and the very large range of temperature is used to deduce a reliable temperature dependence of the thermophysical property data.

2. EXPERIMENTAL METHODS

2.1. Levitation Setup

Figure 1 presents a schematic levitation setup. Iron drops approximately 3 mm in diameter are levitated on a stream of $\text{Ar} : 10\% \text{H}_2$ mixture flowing at 1 or two liters per minute in order to prevent any oxidation. They are melted by continuous CO_2 laser radiation ($\lambda = 10.86 \mu\text{m}$, maximum power = 800 W), forming almost perfect and very stable liquid spheres.

The determination of properties are carried out using a three-colour pyrometer working at 0.4, 0.55, and $0.8 \mu\text{m}$ and a digital high speed camera able to record 2728 frames at a maximum speed of 1000 frames per second. A $/\text{ZrO}_2\text{-Y}_2\text{O}_3/\text{Pd}:\text{PdO}$ electrolytic cell heated at 650°C is used to determine the composition of the $\text{H}_2/\text{H}_2\text{O}$ mixture in the flowing gas.

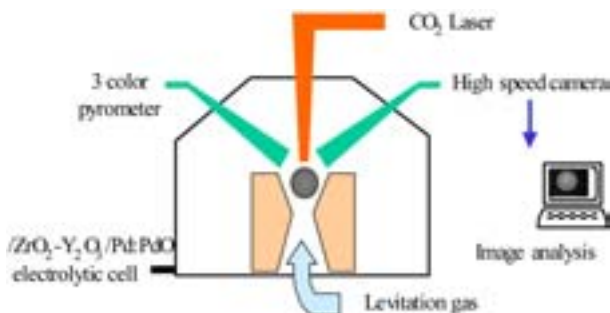


Fig. 1. Experimental setup.

2.2. Samples

Iron with a purity of 99.99% from Chempur (Karlsruhe, Germany) is directly melted in the levitation device to form drops with masses between 43 and 140 mg.

2.3. Calibration of Pyrometers

The output voltage V of the electron photomultiplier receiving filtered light at a wavelength λ is related to the temperature T through the Wien approximation of the Planck relation:

$$V = k_\lambda \exp\left(\frac{-C_2}{\lambda T}\right) \quad (1)$$

where $C_2 = 1.4388 \times 10^{-2} \text{ m} \cdot \text{K}$ (second Planck's radiation constant).

The calibration consists of adjusting the k_λ value to relate V to some known temperature. Actually, k_λ is the product of two terms: $k_\lambda = k_0 \varepsilon_\lambda$, k_0 is a constant related to the geometry of the optical setup as well as the photomultiplier performance, and ε_λ is the normal spectral emissivity of the sample material at λ .

k_0 has been determined from the voltage $V_{\text{Al}_2\text{O}_3}$ of each pyrometer on the solidification plateau of freely cooling liquid alumina at $T_m = 2327 \text{ K}$ and $\varepsilon_\lambda = 0.92$ in the visible region [12]. The transparency of solid alumina permits to get the light coming from the liquid inside the solidifying drop.

The emissivity of liquid iron cannot be obtained directly from the solidification plateau of free cooling liquid iron because contrary to alumina iron is opaque in the visible wavelengths. It is then necessary to get it from the emissivity of iron surface during melting. We have performed an experiment to compare the emissivity of the solid and liquid iron at the melting point. It consists of heating slowly a solid levitating iron drop, observing melting with a $0.75 \mu\text{m}$ pyrometer and then cutting off the laser to obtain a solidification plateau of the undercooled liquid. Figure 2 indicates small difference of the temperature of liquid and solid iron at 1808 K.

This result indicates that we introduce only a small error (1%) in temperature measurement by neglecting the emissivity difference between solid and liquid. In practice, we have used cooling curves to calibrate the three pyrometers (Fig. 3). Results indicate good consistency of the three pyrometers up to high temperatures and emissivities of solid iron of 0.54 at $0.4 \mu\text{m}$, 0.42 at $0.55 \mu\text{m}$, and 0.40 at $0.8 \mu\text{m}$. If we consider the liquid emissivities of the liquid approximately 5% lower than those of the solid, we obtain values in reasonable agreement with formerly published data [13–15].

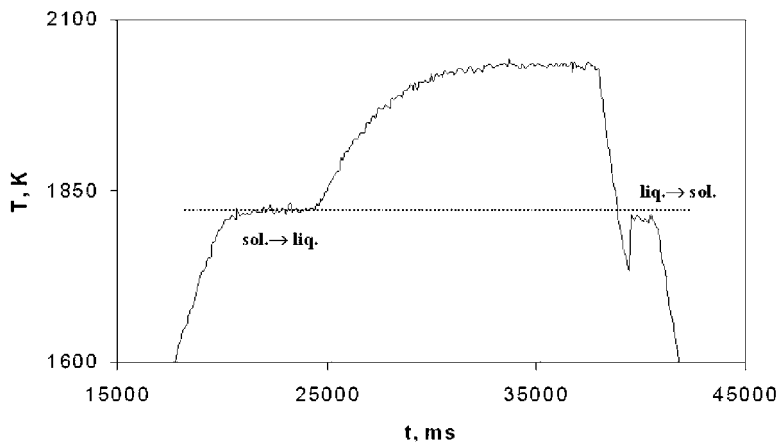


Fig. 2. Apparent temperature of iron obtained with a $0.75 \mu\text{m}$ wavelength pyrometer during heating with CO_2 laser through the melting point followed by the solidification during free cooling.

2.4. Image Analysis

Images of the drop are recorded at 500 or 1000 frames per second. A special interface permits to have the output voltage of one or two pyrometers in every frame. Software is used to convert the image of the drop to a binary image. Diameters, area, and geometrical center of gravity

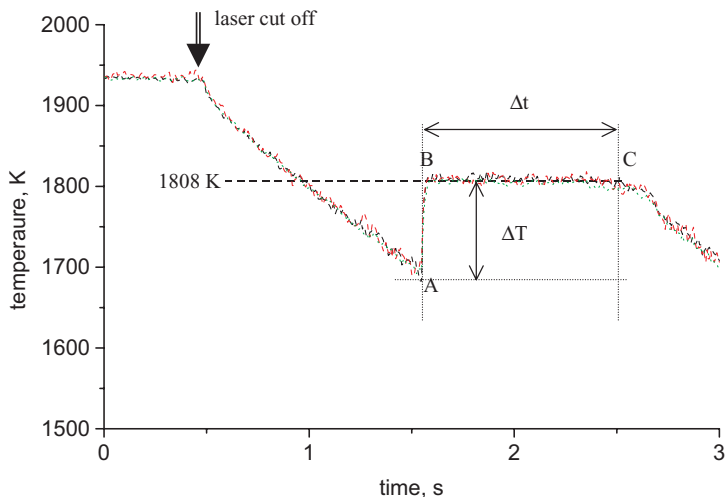


Fig. 3. Cooling curve of iron measured with pyrometers at wavelengths of 0.4, 0.65, and $0.8 \mu\text{m}$.

can be deduced from the approximate circle corresponding to the drop image. These measurements can be converted from pixels to length or surface area by calibrating the setup with a sphere of known diameter.

Fast Fourier transforms of geometrical characteristic values versus time allow are performed to obtain frequencies that are used to determine the surface tension.

3. RESULTS

3.1. Results Deduced from Cooling Curves

A typical free cooling curve obtained by measuring the temperature change of a levitated droplet with time is shown on Fig. 3. It is worth noting that the homogeneous crystallization of the solid is a quite well defined event corresponding to the temperature plateau at $T_m = 1808$ K. Recalescence (observed with the high speed camera) from A to B is quite fast (< 1 ms). It is possible from such a curve to deduce thermodynamic quantities related with to the path going from the undercooled liquid at point A of Fig. 3 to the end of solidification going from point B to point C during the time interval Δt . During that time, the heat exchanged between the drop and its local environment is proportional to its surface area S and the time interval Δt . Then we can write $\Delta Q = kS \Delta t$ because the time to proceed from point A to point B (1 ms) is negligible with respect to the plateau time from B to C. We consider k as an exchange constant which is independent of the size of the drop and is characteristic for the heat exchange coefficient at the melting temperature $T_c = 1808$ K. The same quantity of heat ΔQ is equal to the heat necessary to transform n moles of liquid at T_A to n moles of solid at the melting temperature $T_c = 1808$ K

$$\Delta Q = n(-C_P^L(T_C - T_A) + \Delta H_m) = kS \Delta t. \quad (2)$$

The k constant becomes a k' constant independent of the size of the drop if we express the mole number n and the surface S as a function of the mass of the drop m :

$$\sqrt[3]{m}(T_C - T_A) / \Delta T = \left(\frac{\Delta H_m}{C_P^L} \right) \frac{\sqrt[3]{m}}{\Delta t} + k'. \quad (3)$$

This relation gives an unique relation between $\frac{\sqrt[3]{m}}{\Delta t}$ and $\frac{\sqrt[3]{m}(T_C - T_A)}{\Delta t}$ which is valid for all samples whatever their mass and their degree of undercooling of the liquid is, as long as it is smaller than $T_C - T_A = \frac{\Delta H_m}{C_P^L}$. Values for different experiments performed on drops of various masses ranging from

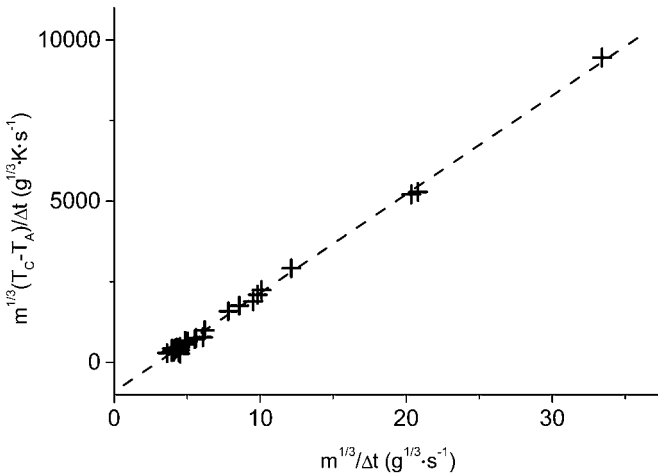


Fig. 4. Linear behavior deduced from heat balance equation during solidification.

43 to 140 mg are presented in Fig. 4. They follow a linear behavior which can be used to deduce the slope $\frac{\Delta H_m}{C_p^l} = 306 \pm 2.5 \text{ K}$.

3.2. Surface Tension

The determination of the surface tension is based on the theory of Lord Rayleigh [16] of the vibrations of a three-dimensional harmonic oscillator. The surface tension σ is the force which determines the spherical shape. It is directly related to a unique characteristic frequency ν for a spherical drop of mass m by

$$\sigma = \frac{3\pi m \nu^2}{8} \quad (4)$$

In practice, Fourier transforms (FFT) show complicated structures of peaks which result from degeneracy splitting of ν due to the various external forces applied to the levitated drop as well as kinematic effects introduced by rotation and precession. It has been recently shown [11] that the analysis of the Fourier transforms of the sum of diameters (or surface area) and that of the difference of perpendicular diameters can be used to deduce relatively easily five characteristic frequencies, namely, ν_k with $k = -2, -1, 0, 1, 2$, as well as the rotation frequency Ω_R and the precession frequency Ω_P of the drop. Figure 5 shows an example of the Fourier transform of a

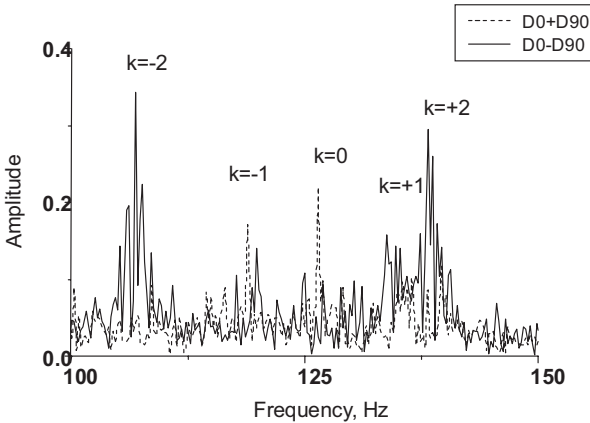


Fig. 5. Characteristic FFT result of the sum and the difference of orthogonal diameters showing five peaks' behavior of liquid iron drop.

liquid iron drop. Oscillation peaks assignment is performed according to azimuthal symmetry of oscillations. The $k = -2$ and $k = +2$ vibration modes appear as strong peaks in $D0 - D90$ FFT with $\nu_2 - \nu_{-2} = 4\Omega_r$. The $k = 0$ oscillation mode is strong the main peak of $D0 + D90$ FFT. The $k = -1$ and $k = +1$ oscillation modes appear as strong weak peaks in $D0 + D90$ and $D0 - D90$ FFTs with $\nu_1 - \nu_{-1} = 2\Omega_r$.

It has also been shown [11] that, in aerodynamic levitation, the surface tension is obtained to a very good approximation by the formula:

$$\sigma = \frac{3\pi m}{40} \sum_{-2}^2 \nu_k^2 \quad (5)$$

We have used this method to obtain surface tensions of liquid iron with a precision of 2% between 1750 and 2500 K. The higher limit of temperature is mainly due to vaporization effects of the drop. Results are shown in Fig. 6 and compared to results of other authors [1–6]. They follow a straight line behaviour, which is given by

$$\sigma \text{ (mN} \cdot \text{m}^{-1}\text{)} = (1888 \pm 31) - (0.285 \pm 0.015) (T - T_m). \quad (6)$$

3.3. Density

Density measurements of levitating liquids in aerodynamic devices were first described by Granier and Heurtault [9]. It is based on the

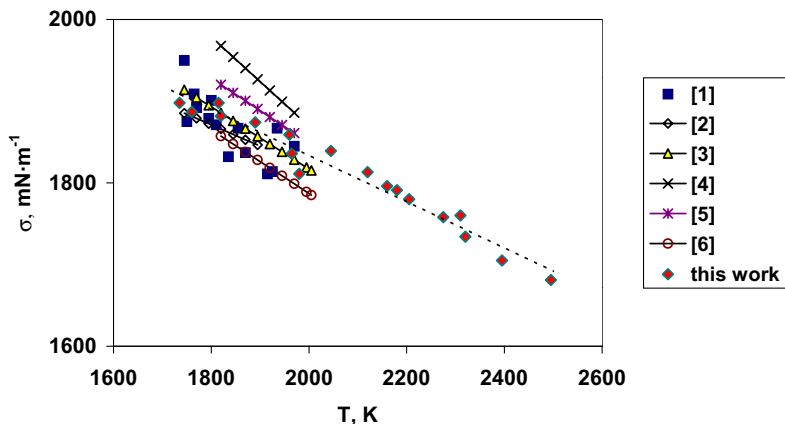


Fig. 6. Surface tension of liquid iron at various temperatures.

approximation of perfect sphericity of the liquid drop; thus, the density is given by $\rho = \frac{3m\sqrt{4\pi}}{S^{3/2}}$ where m is the mass of the drop measured immediately after the experiment and S is the surface area of the projection of the liquid drop on a plane (the image of the camera). Two alternative experimental methods are possible. One consists of measuring surface areas of the 2728 images with the laser impinging on the drop. Another is the measure of surface areas during free cooling. Both methods have been used, and results are shown in Fig. 7 and are compared to results of other authors [17–25].

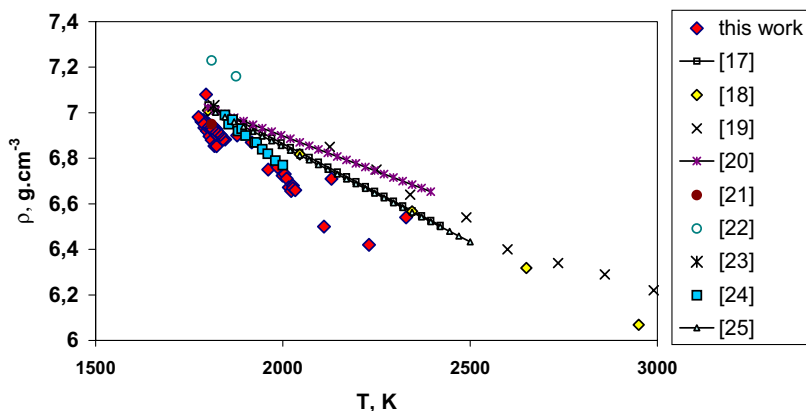


Fig. 7. Density of liquid iron at various temperatures.

4. DISCUSSION

Iron properties have been extensively studied in the past. Comparison of our results with these previous studies are valuable since they can be used to validate the contactless experimental methods used in this study which are still under development.

If we compare $\frac{\Delta H_m}{C_p^\ell} = 306 \pm 2.5$ K obtained by us with the value of (300 ± 14) K obtained from more recent JANAF [26] recommended values of $\Delta H_m = 3300 \pm 100$ cal·mol⁻¹ and $C_p^\ell = 11 \pm 0.2$ cal·mol⁻¹·K⁻¹, the agreement is excellent and confirms both our methodology and the choices of JANAF reviewers ($\frac{\Delta H_m}{C_p^\ell}$ values from literature vary from 231 to 457 K).

Surface tensions from the literature [1–6] are plotted in Fig. 6 and compared with our data. The first striking point is the generally good agreement of data. The temperature dependence of the surface tension is more dispersed, probably because of the relatively small temperature range and the scatter of surface tension data of most authors. Our results are particularly consistent since they were obtained on drops of different masses giving very well aligned temperature dependence and very small scatter. These data indicate that aerodynamic levitation is a good technique for surface tension measurements. They show good agreement with former results on liquid iron as well as on liquid nickel [11] with better consistency over a very large range of temperature.

Densities, on the contrary, are poorly aligned (see Fig. 7). Comparison with former results [17–25] is relatively good, although the data that we present are systematically somewhat lower than values published in the literature (1%). These results probably indicate that progress can already be done made to improve the quality of density measurements. The weak point of the methodology that we used lies in the fact that we considered the drop to be perfectly spherical. This assumption has clearly no reason to be true. In fact, Fourier transforms of the drop vibrations show frequency splitting of the three fundamental modes (see Fig. 5) which is a clear indication of asphericity. Nevertheless, the deviation from sphericity for liquid iron is about the same order of magnitude (1 or 2%) as the precision of the surface tension measurements. Since splitting of vibration frequencies is directly proportional to deformation [27], it seems hopeless unreasonable to correct the data on liquid iron for nonspherical effects.

5. CONCLUSION

The present study confirms and extends the available data on liquid iron to higher temperatures. A recalescence phenomenon was shown to be an accurate method to determine the ratio of the enthalpy of melting to the

heat capacity of the liquid. Particularly important is the high accuracy of the surface tension measurement which will permit future reliable measurements on other high-temperature materials. On the contrary, density measurement may be improved by analyzing the true shape of levitating drops.

REFERENCES

1. S. Sauerland, *Ph.D., Rheinisch-Westfälische Technische Hochschule Aachen* (1993).
2. I. Seihan and I. Egry, *Int. J. Thermophys.* **20**:1017 (1999).
3. R. A. Eichel and I. Egry, *Z. Metallkd.* **90**:371 (1999).
4. B. J. Keene, K. C. Mills, and R. F. Brooks, *Mat. Sci. and Tech.* **1**:568 (1985).
5. H. K. Lee, M. G. Froberg, and J. P. Hajra, *Steel Research* **64**:191 (1993).
6. B. J. Keene, *Int. Mat. Rev.* **38**:157 (1993).
7. P. C. Nordine and R. M. Atkins, *Rev. Sci. Instr.* **53**:1456 (1982).
8. W. K. Rhim, S. K. Chung, A. J. Rulinson, and R. E. Spjut, *Int. J. Thermophys.* **18**:459 (1997).
9. B. Granier and S. Heurtault, *Rev. Int. Hautes Tempér. Réfract. Fr.* **20**:61 (1983).
10. B. Glorieux, F. Millot, J. C. Rifflet, and J. P. Coutures, *Int. J. Thermophys.* **20**:1085 (1999).
11. F. Millot, J. C. Rifflet, G. Wille, V. Sarou-Kanian, and B. Glorieux *J. Amer. Ceram. Soc.* **85**:187 (2002).
12. F. Millot, B. Glorieux, and J. C. Rifflet, *Prog. Astronaut. And Aeronaut.* **185**:777 (2000).
13. S. Krishnan, K. J. Yugawa, and P. C. Nordine, *Phys. Rev. B* **55**:8201 (1997).
14. L. S. Dubrovinsky and S. K. Saxena, *High Temp.-High Press.* **31**:393 (1999).
15. E. Kaschnitz, J. L. McClure, and A. Cezairliyan, *High Temp.-High Press.* **29**:103 (1997).
16. Lord Rayleigh, *Proc. Roy. Soc. London* **29**:71 (1879).
17. T. Saito, Y. Shiraishi, and Y. Sakuma, *Trans. ISIJ* **9**:118 (1969).
18. M. Beutl, G. Pottlacher, and H. Jäger, *Int. J. Thermophys.* **15**:1323 (1994).
19. R. S. Hixson, M. A. Winkler, and M. L. Hodgdon, *Phys. Rev. B* **42**:6485 (1990).
20. W. D. Drotning, *High Temp.-High Press.* **13**:441 (1981).
21. C. H. Desch and B. S. Smith, *J. Iron Steel Inst.* **119**:358 (1929).
22. C. Benedicks, N. Ericsson, and G. Ericson, *Arch. Eisenhüttenw.* **3**:473 (1930).
23. V. H. Stott and J. H. Rendall, *J. Iron Steel Inst.* **175**:374 (1953).
24. L. D. Lucas, *Compt. Rend. Acad. Sci.* **250**:1850 (1960).
25. A. D. Kirshenbaum and J. A. Cahill, *Trans. ASM* **56**:281 (1963).
26. *JANAF Thermochemical Tables*, 3rd ed., Vol. 14, Sup. 1 (1985).
27. D. L. Cummings and D. A. Blackburn, *J. Fluid Mech.* **224**:395 (1991).